Journal of Pharmaceutical and Biomedical Analysis 53 (2010) 799–803

Contents lists available at ScienceDirect

Journal of Pharmaceutical and Biomedical Analysis

journal homepage: www.elsevier.com/locate/jpba

Short communication

Curve-fitting FTIR studies of loratadine/hydroxypropyl-β-cyclodextrin inclusion complex induced by co-grinding process

Shan-Yang Lin[a,*], Cheng-Hung Hsu[a], Ming-Thau Sheu[b]

[a] Lab. Pharm. Biopharm., Department of Biotechnology, Yuanpei University, Hsin Chu, Taiwan, ROC
[b] College of Pharmacy, Taipei Medical University, Taipei, Taiwan, ROC

ARTICLE INFO

Article history:
Received 20 February 2010
Received in revised form 12 June 2010
Accepted 14 June 2010
Available online 19 June 2010

Keywords:
Loratadine
Hydroxypropyl-β-cyclodextrin
Inclusion complex
Co-grinding
FTIR
DSC
Curve-fitting

ABSTRACT

The formation steps of inclusion complex caused by co-grinding loratadine (LOR) and hydroxypropyl-β-cyclodextrin (HP-β-CD) with a molar ratio of 1:1 or 1:2 were quantitatively investigated by Fourier transform infrared (FTIR) spectroscopy with curve-fitting analysis and differential scanning calorimetry (DSC). The phase solubility study and the co-evaporated solid products of the mixture of LOR and HP-β-CD were also examined. The result indicates that the aqueous solubility of LOR was linearly increased with the increase of HP-β-CD concentrations, in which the phase solubility diagram was classified as A_L type. The higher apparent stability constant ($2.22 \times 10^4\ M^{-1}$) reveals that the inclusion complex formed between LOR and HP-β-CD was quite stable. The endothermic peak at 134.6 °C for the melting point of LOR gradually disappeared from DSC curves of LOR/HP-β-CD coground mixtures by increasing the cogrinding time, as the disappearance of the co-evaporated solid products. The disappearance of this endothermic peak from LOR/HP-β-CD coground mixture or the co-evaporated solid products was due to the inclusion complex formation between LOR and HP-β-CD after cogrinding process or evaporation. Moreover, IR peaks at 1676 cm^{-1} down-shifted from 1703 cm^{-1} (C=O stretching) and at 1235 cm^{-1} upper-shifted from 1227 cm^{-1} (C–O stretching) related to LOR in the inclusion complex were observed with the increase of cogrinding time, but the peak at 1646 cm^{-1} due to O–H stretching of HP-β-CD was shifted to 1640 cm^{-1}. The IR spectrum of 15 min-coground mixture was the same as the IR spectrum of the co-evaporated solid product, strongly indicating that the grinding process could cause the inclusion complex formation between LOR and HP-β-CD. Three components (1700, 1676, and 1640 cm^{-1}) and their compositions were certainly obtained in the 1740–1600 cm^{-1} region of FTIR spectra for the LOR/HP-β-CD coground mixture and the co-evaporated solid products by curve-fitting analysis. The component of 1700 cm^{-1} detected was due to the un-included LOR in the inclusion complex. This implies that FTIR spectroscopy with curve-fitting analysis might be useful for discriminating the components and compositions in the inclusion complex.

1. Introduction

Loratadine (LOR, Fig. 1) is a potent long-acting second-generation tricyclic H_1 antihistamine for the symptomatic relief of allergic disorders without significant central and autonomic nervous side effects [1,2]. LOR has also been widely combined with pseudoephedrine sulfate as an over-the-counter medicine in the relief of symptoms associated with allergic rhinitis and common cold usually including nasal congestion, sneezing, rhinorrhea, pruritus and lacrimation [3,4]. It has been reported that LOR belongs to the class II of Biopharmaceutical Classification System (BSC), since LOR has a poor solubility in water but is absorbed rapidly after oral administration in human [5]. Due to the poor water-soluble property and very low dissolution rate of LOR, its bioavailability exhibits high intra and inter subject variability [6,7]. Therefore, how to improve the solubility of LOR plays an important role in the pharmaceutical formulation design.

Several techniques have been attempted to improve the solubility and dissolution rate of LOR by using solid dispersion, micellar solubilization or inclusion complex formation [8–12]. The inclusion complex of LOR with β-cyclodextrin, hydroxypropyl-β-cyclodextrin (HP-β-CD) or dimethyl-β-CD had been extensively studied by kneading, spray-drying, freeze-drying and microwave irradiation [10–12], but the conventional grinding process always used in pharmaceutical industry is still lacking in the available application. In the present investigation, the progressive steps of inclusion complex formation caused by co-grinding LOR with HP-β-CD were quantitatively investigated by Fourier transform

* Corresponding author. Tel.: +886 03 5381183x8157; fax: +886 03 6102328.
E-mail address: sylin@mail.ypu.edu.tw (S.-Y. Lin).

0731-7085/$ – see front matter © 2010 Elsevier B.V. All rights reserved.
doi:10.1016/j.jpba.2010.06.010

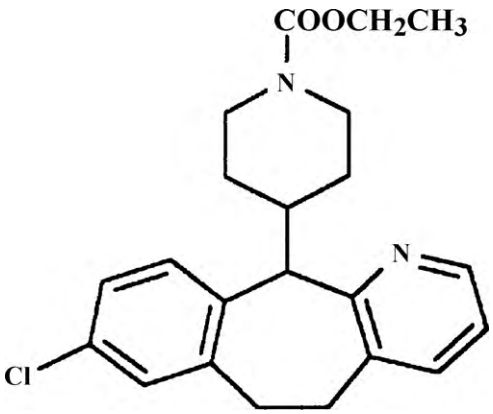

Fig. 1. Chemical structure of loratadine.

infrared spectroscopy with curve-fitting analysis and thermal analysis.

2. Experimental

2.1. Materials

Loratadine (LOR) was of pharmaceutical grade (Jai Radhe Sales, Gujarat, India) and used without further purification. Hydroxypropyl-β-cyclodextrin (HP-β-CD) was obtained from Roquette Freres, Lestrem, France. All the other materials were of analytical reagent grade.

2.2. Phase solubility study

Solubility measurement was carried out at 25 ± 0.5 °C according to the method of Higuchi and Connors [13]. Different aqueous concentrations of HP-β-CD in double distilled water (pH 5.6) were previously prepared. An excess amount of LOR was added to each solution, and then shaken at room temperature for 72 h. After 72 h, all the suspensions were filtered using 0.45 μm membrane filters. Each filtrate was appropriately diluted with 50% alcoholic water and measured by UV spectrophotometer at 248 nm. The presence of the HP-β-CD did not interfere with the spectrophotometric assay. Each experiment was performed in triplicate and the mean was obtained. An apparent stability constant was calculated from the initial straight line portion of the phase solubility diagram.

2.3. Preparation of the co-evaporated solid products

The co-evaporated solid products of LOR and HP-β-CD with a molar ratio of 1:1 or 1:2 were prepared by solvent evaporation method. Both samples with different molar ratios were dissolved in ethyl alcohol and then evaporated at room temperature. The dried samples were washed with acetone and then dried at 50 °C. The LOR in the absence of HP-β-CD was also performed.

2.4. Preparation of co-ground mixtures of LOR and HP-β-CD with different molar ratios

The co-ground mixtures of LOR and HP-β-CD in the 1:1 or 1:2 molar ratio were respectively prepared in an oscillatory ball mill (Mixer Mill MM301, Retsch GmbH & Co., Germany) at 15 Hz for different times. About 0.2 g powder sample was placed in a 25 ml volume stainless steel milling jar containing two 15 mm diameter stainless steel balls. During co-grinding, the sample was withdrawn at prescribed intervals for further examination.

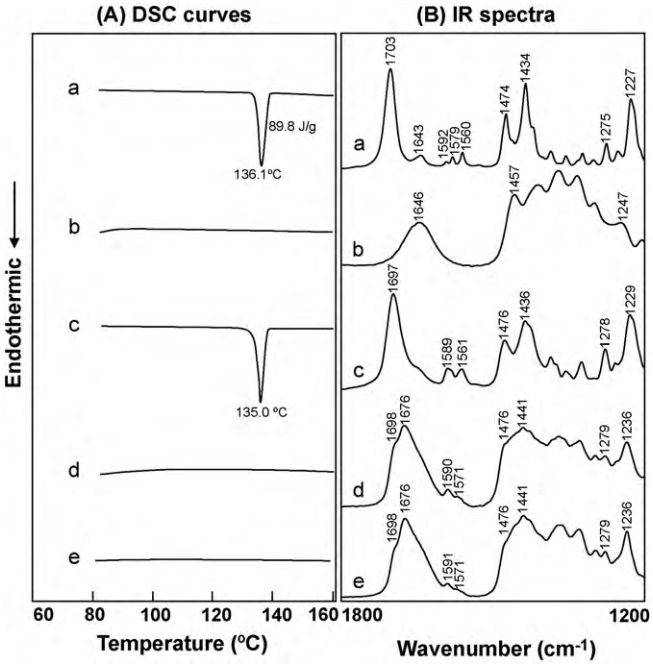

Fig. 2. DSC curves and FTIR spectra of LOR (a, c), HP-β-CD (b) and the solid products (d, e) after co-evaporation.
Key: (a) intact LOR; (b) intact HP-β-CD; (c) LOR evaporated from ethyl alcohol; LOR/HP-β-CD with a molar ratio of 1:1 (d) or 1:2 (e).

2.5. Identification of each sample

Each sample was determined by using a differential scanning calorimetry (DSC, TA Instruments, Inc., New Castle, DE) at a heating rate of 3 °C/min with an open pan system in a stream of N_2 gas, and an Fourier transform infrared (FTIR) microspectroscopy (IRT-5000-16/FTIR-6200, Jasco Co., Tokyo, Japan) equipped with a mercury cadmium telluride (MCT) detector via a transmission technique [14,15]. All the FTIR spectra were obtained at a 4 cm^{-1} resolution and at 100 scans. Both determinations were undertaken at 25 ± 2 °C and 65 ± 5% RH condition.

2.6. Application of curve-fitting analysis to FTIR spectra

The components and relative compositions of each sample were estimated quantitatively in the 1740–1600 cm^{-1} region of FTIR spectra by a curve-fitting algorithm with a Gaussian–Lorenzian function [16,17]. The best curve-fitting procedure was performed by iterative fits toward a minimum standard error. Because the analysis depends on the positions and intensities of the components of the contour, substantial attention was paid to obtaining the best possible fit with the minimum number of component bands. The relative proportion of a component was computed to be the fractional area of the corresponding peak, divided by the sum of areas of all the peaks.

3. Results and discussion

3.1. Identification and characterization of LOR and the evaporated solid products

Fig. 2 shows the DSC curves and FTIR spectra of LOR, HP-β-CD and the solid products after co-evaporation. It is apparent that only one sharp endothermic peak at 136.1 °C with an enthalpy of 89.8 J/g was observed in DSC thermogram of intact LOR. This endothermic peak was due to the melting point of LOR. The FTIR

spectrum of intact LOR is also displayed in Fig. 2. Several characteristic IR absorption bands and their assignments of LOR are shown as follows: 1703 cm^{-1} (C=O of ester), 1560 and 1474 cm^{-1} (stretching vibrations of benzene ring), and 1227 cm^{-1} (C–O stretching), respectively [10,12,18]. On the other hand, there was lack of endothermic peak within the temperature range of 30–160 °C for intact HP-β-CD. The IR peak at 1646 cm^{-1} may be attributed to the OH groups in the glucose moieties of HP-β-CD [19]. In addition, there was no significant change in DSC curve and FTIR spectrum for the evaporated LOR alone, as compared with intact LOR. However, the DSC curves and FTIR spectra of solid products containing LOR and HP-β-CD in a 1:1 or 1:2 molar ratio indicate different patterns, in which no any endothermic peak was observed for both solid products but two new peaks at 1676 and 1236 cm^{-1} were found in the IR spectra. The disappearance of an endothermic peak in DSC curve and a new IR spectral peak formation might be explained by the inclusion complex formation between LOR and HP-β-CD. Due to the inclusion complex formation, the characteristic bands at 1703 and 1227 cm^{-1} of LOR were down-shifted to 1676 cm^{-1} and upper-shifted to 1236 cm^{-1}, respectively.

3.2. Phase solubility study

Phase solubility study of LOR-HP-β-CD systems in water at 25 °C reveals that the aqueous solubility of LOR was linearly increased with an increase of the HP-β-CD concentrations. The linear plot has a slope value of 0.1276 with a correlation coefficient of 0.9984. The phase solubility diagram can be classified as A_L phase diagram, according to the classification of Higuchi and Connors [13]. This indicates the formation of soluble binary complexes of probable 1:1 stoichiometry. The apparent stability constant (K_c) was estimated from the slope of the linear plot of phase solubility diagram according to the equation $K_c = \text{slope}/S_o\ (1 - \text{slope})$, where S_o is the solubility of LOR in the absence of HP-β-CD. The value of K_c was 2.22 × x10^4 M^{-1}. The higher K_c value reveals that the inclusion complex formed between LOR and HP-β-CD was quite stable.

3.3. Co-grinding effect on the inclusion complex formation of LOR with HP-β-CD

Fig. 3 displays time-dependent changes in DSC curves and IR spectra of coground mixtures of LOR and HP-β-CD with a 1:1 molar ratio. It is evident that the endothermic peak at 134.6 °C for LOR decreased with the increasing grinding time. This endothermic peak disappeared beyond 7 min-cogrinding process, as it did with the evaporated solid products. The disappearance of this endothermic peak might be due to the inclusion complex formation by cogrinding LOR with HP-β-CD. This was also confirmed from the changes in FTIR spectra. After cogrinding for 5 min, a shoulder at 1678 cm^{-1} was observed. By continuing the cogrinding process, the shoulder at 1678 cm^{-1} was shifted to a predominant peak at 1676 cm^{-1}. In addition, the peak at 1229 cm^{-1} assigned to C–O stretching vibration was also shifted to 1236 cm^{-1}. The IR spectrum of 15 min-coground mixture was the same as the IR spectrum of the co-evaporated solid product as shown in Fig. 2. This strongly demonstrates that the co-grinding process could cause the inclusion complex formation between LOR and HP-β-CD.

In order to understand the effect of additional amount of HP-β-CD, the coground mixture of LOR and HP-β-CD with a molar ratio of 1:2 was also carried out. Fig. 4 reveals time-dependent changes in DSC curves and IR spectra of coground mixtures of LOR and HP-β-CD with a 1:2 molar ratio. Obviously, the endothermic peak at 134.9 °C was slowly shifted to lower temperature with the increase of co-grinding time. The changes in IR spectra were also slow down with co-grinding time. This was significantly different from that of the results in Fig. 3. However, the DSC curve and IR spectrum of 15 min-coground mixture of LOR and HP-β-CD with a 1:2 molar ratio were also similar to that of the results of 15 min-coground mixture of LOR and HP-β-CD with a 1:1 molar ratio and both the evaporated solid products. Although the inclusion complex was also formed in the 15 min-coground mixture of LOR and HP-β-CD with a 1:2 molar ratio, the excess amount of HP-β-CD might delay the inclusion complex formation in the mixture during the cogrinding process.

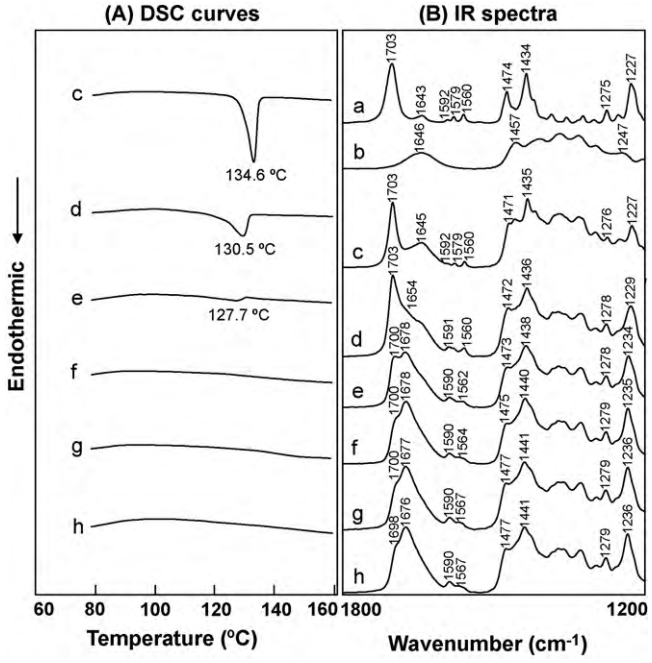

Fig. 3. Time-dependent changes in DSC curves and IR spectra of coground mixtures of LOR and HP-β-CD with a 1:1 molar ratio
Key: (a) intact LOR; (b) intact HP-β-CD; cogrinding time (min): (c) 0; (d) 3; (e) 5; (f) 7; (g) 10; (h) 15.

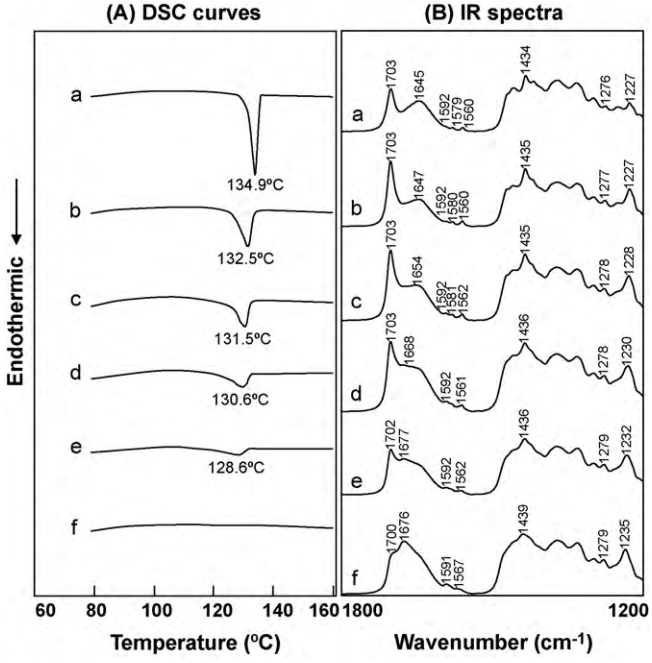

Fig. 4. Time-dependent changes in DSC curves and IR spectra of coground mixtures of LOR and HP-β-CD with a 1:2 molar ratio.
Key: cogrinding time (min): (a) 0; (b) 3; (c) 5; (d) 7; (e) 10; (f) 15.

3.4. Quantitative analysis of the time-dependent inclusion complex formation after co-grinding

It is well known that the curve fitting analysis is an effective means for estimating the number of bands, and their positions and compositions in the spectra [20,21]. Here, the curve-fitting program was combined with a nonlinear deconvolution technique to probe the nature and extent of structural changes in the IR spectra of different samples. The IR spectral region of 1740–1600 cm^{-1} was selected, since the most marked alteration was found in this region [16,17].

The best-fitted FTIR spectra and the deconvoluted components in the 1740–1600 cm^{-1} region for LOR, HP-β-CD and the co-evaporated solid products are indicated in Fig. 5.

It is evident that the assignment and composition of the curve-fitted IR spectra for each sample were obtained as follows: 1703 cm^{-1} (93.2%) and 1643 cm^{-1} (6.8%) for intact LOR; 1646 cm^{-1} (100%) for intact HP-β-CD; 1700 cm^{-1} (9.7%), 1676 cm^{-1} (76.5%) and 1640 cm^{-1} (13.8%) for the co-evaporated solid product with a 1:1 molar ratio of LOR and HP-β-CD; 1700 cm^{-1} (2.7%), 1676 cm^{-1} (68.3%) and 1640 cm^{-1} (29.1%) for the co-evaporated solid product with a 1:2 molar ratio of LOR and HP-β-CD, respectively. Three components were certainly detected in the IR spectrum of the co-evaporated solid products. The best-fitting results reveal that the predominant peak at 1703 cm^{-1} assigned to C=O group of ester for LOR was markedly shifted to 1677 (1676) cm^{-1} after formation of inclusion complex by using a co-evaporation method. Moreover, the peak at 1646 cm^{-1} due to the hydroxyl groups in the glucose moieties of HP-β-CD was also shifted to 1640 cm^{-1}. This suggests that both peaks were the unique peaks for inclusion complex formation between LOR and HP-β-CD. It is also found that the composition of the peak at 1700 cm^{-1} corresponded to the un-included C=O group of LOR was reduced from 9.7% to 2.6% with the increase of HP-β-CD added, suggesting the more content of inclusion complex was formed in the co-evaporated solid product with a 1:2 molar ratio of LOR and HP-β-CD.

Fig. 6 or 7 displays time-dependent inclusion complex formation between LOR and HP-β-CD with either 1:1 or 1:2 molar ratio during cogrinding process. Obviously, the changes in IR spectra and the compositions of three components were observed for both coground mixtures with the increase of cogrinding time. It clearly indicates that after 15 min-cogrinding course the coground mixture of LOR and HP-β-CD with either 1:1 or 1:2 molar ratio exhibited similar compositions of inclusion complex. This was somewhat different from that of inclusion complex prepared by co-evaporation method, although the results of DSC and IR spectra were almost the same. This strongly implies that the curve-fitting analysis may be used to obtain the reliable quantitative information about the inclusion complex formation.

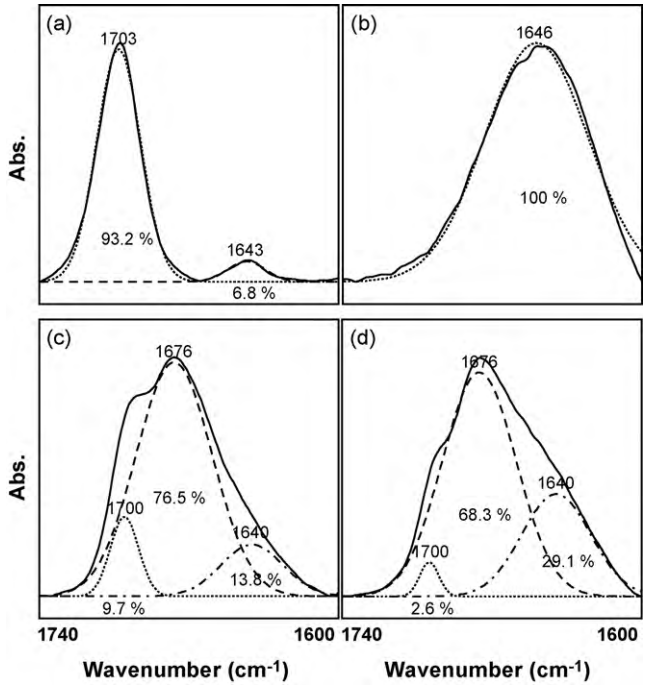

Fig. 5. The best-fitted FTIR spectra and the deconvoluted components in the 1740–1600 cm^{-1} region for LOR, HP-β-CD and the co-evaporated solid products. *Key*: (a) intact LOR; (b) intact HP-β-CD; LOR/HP-β-CD with a molar ratio of 1:1 (c) or 1:2 (d).

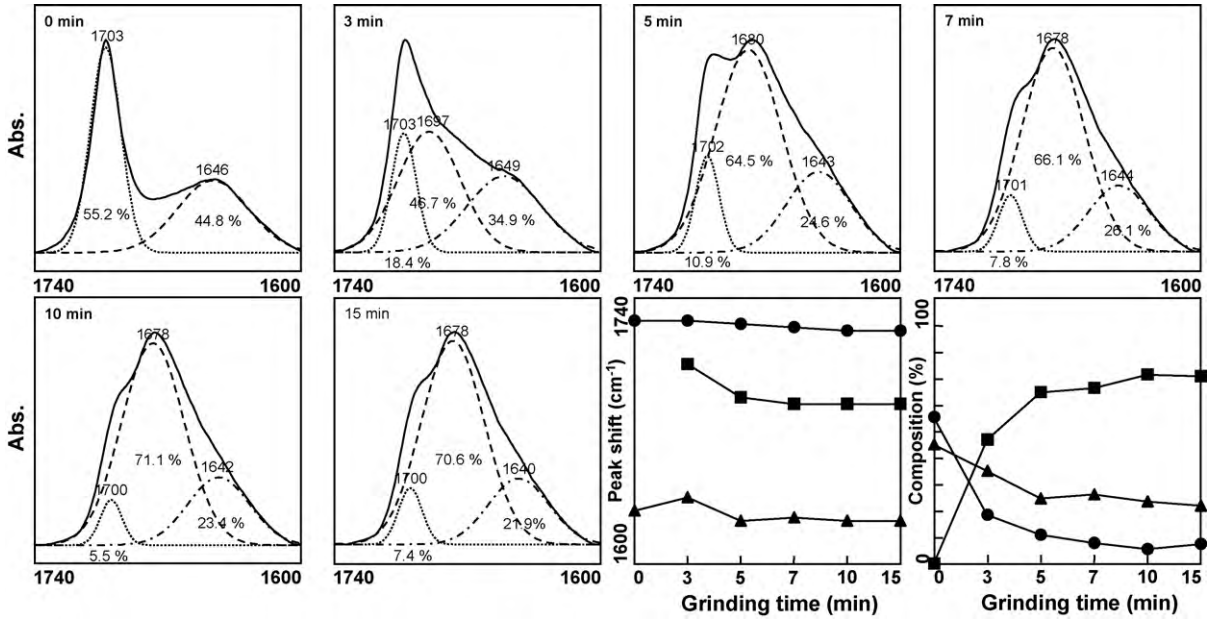

Fig. 6. Time-dependent inclusion complex formation between LOR and HP-β-CD with a 1:1 molar ratio during cogrinding process.

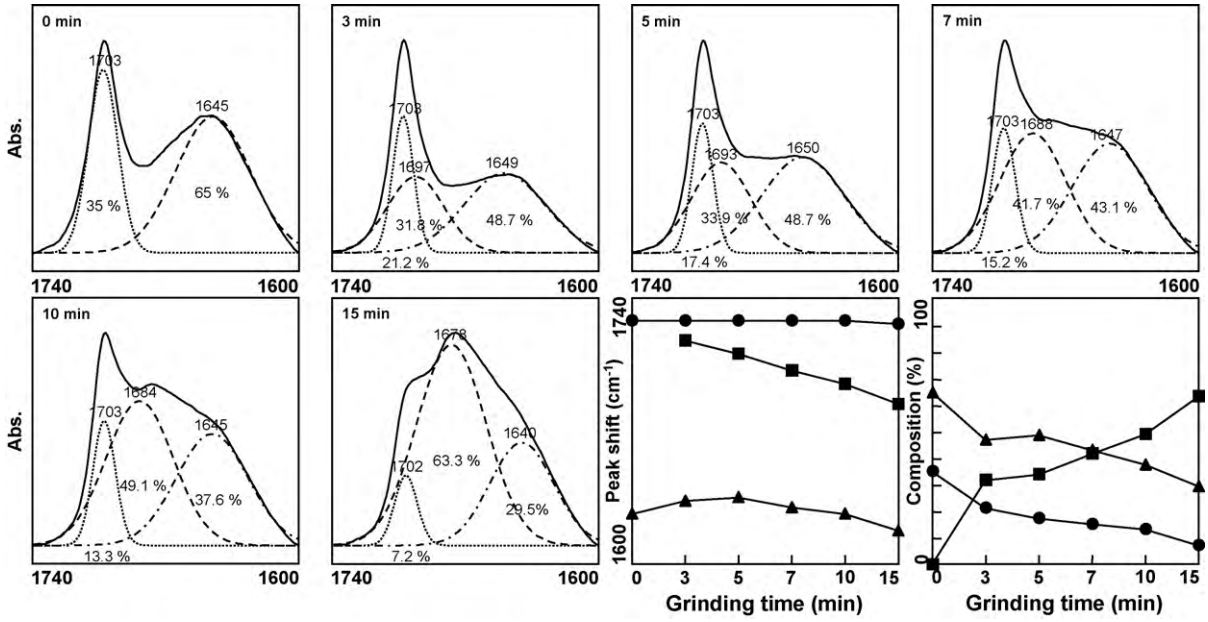

Fig. 7. Time-dependent inclusion complex formation between LOR and HP-β-CD with a 1:2 molar ratio during cogrinding process.

In conclusion, inclusion complex between LOR and HP-β-CD was easily induced by co-grinding process. The FTIR spectroscopy with curve-fitting analysis might be availably used to discriminate the components and compositions in the inclusion complex.

References

[1] G.M. Walsh, Second-generation antihistamines in asthma therapy: is there a protective effect? Am. J. Respir. Med. 1 (2002) 27–34.

[2] A. Banerji, A.A. Long, C.A. Camargo Jr., Diphenhydramine versus nonsedating antihistamines for acute allergic reactions: a literature review, Allergy Asthma Proc. 28 (2007) 418–426.

[3] L.E. Mansfield, Once-daily immediate-release fexofenadine and sustained-release pseudoephedrine combination: a new treatment option for allergic rhinitis, Expert Opin. Pharmacother. 7 (2006) 941–951.

[4] R. Anolik, Desloratadine and pseudoephedrine combination therapy as a comprehensive treatment for allergic rhinitis and nasal congestion, Expert Opin. Drug Metab. Toxicol. 5 (2009) 683–694.

[5] M.Z. Khan, D. Rausl, R. Zanoski, S. Zidar, J.H. Mikulcić, L. Krizmanić, M. Eskinja, B. Mildner, Z. Knezević, Classification of loratadine based on the biopharmaceutics drug classification concept and possible in vitro-in vivo correlation, Biol. Pharm. Bull. 27 (2004) 1630–1635.

[6] P. Patil, A. Paradkar, Porous polystyrene beads as carriers for self-emulsifying system containing Loratadine, AAPS PharmSciTech. 7 (2006) E28.

[7] D.I. Sora, S. Udrescu, V. David, A. Medvedovici, Validated ion pair liquid chromatography/fluorescence detection method for assessing the variability of the loratadine metabolism occurring in bioequivalence studies, Biomed. Chromatogr. 21 (2007) 1023–1029.

[8] J.A. Baird, L.S. Taylor, Evaluation and modeling of the eutectic composition of various drug-polyethylene glycol solid dispersions, Pharm. Dev. Technol. (2010), Feb 9. [Epub ahead of print].

[9] G. Popović, M. Cakar, D. Agbaba, Acid–base equilibria and solubility of loratadine and desloratadine in water and micellar media, J. Pharm. Biomed. Anal. 49 (2009) 42–47.

[10] A. Nacsa, R. Ambrus, O. Berkesi, P. Szabó-Révész, Z. Aigner, Water-soluble loratadine inclusion complex: analytical control of the preparation by microwave irradiation, J. Pharm. Biomed. Anal. 48 (2008) 1020–1023.

[11] L. Omar, M.I. El-Barghouthi, N.A. Masoud, A.A. Abdoh, M.M. Al Omari, M.B. Zughul, A.A. Badwan, Inclusion complexation of loratadine with natural and modified cyclodextrins: phase solubility and thermodynamic studies, J. Solution Chem. 36 (2007) 605–616.

[12] Á. Nacsa, O. Berkesi, P. Szabó-Révész, Z. Aigner, Achievement of pH-independence of poorly-soluble, ionizable loratadine by inclusion complex formation with dimethyl-β-cyclodextrin, J. Inclusion Phenom. Macrocyclic Chem. 64 (2009) 249–254.

[13] T. Higuchi, K.A. Connors, Phase-solubility techniques, Adv. Anal. Chem. Instr. 4 (1965) 117–212.

[14] S.Y. Lin, W.T. Cheng, S.L. Wang, Thermodynamic and kinetic characterization of polymorphic transformation of famotidine during grinding, Int. J. Pharm. 318 (2006) 86–91.

[15] G.Y. Gao, S.Y. Lin, Thermodynamic investigations of nitroxoline sublimation by simultaneous DSC-FTIR method and isothermal TG analysis, J. Pharm. Sci. 99 (2010) 255–261.

[16] W.T. Cheng, S.Y. Lin, S.L. Wang, Differential scanning calorimetry with curve-fitting program used to quantitatively analyze the polymorphic transformation of famotidine in the compressed compact, Drug Dev. Ind. Pharm. 34 (2008) 1368–1375.

[17] T.C. Hu, S.L. Wang, T.F. Chen, S.Y. Lin, Hydration-induced proton transfer in the solid state of norfloxacin, J. Pharm. Sci. 91 (2002) 1351–1357.

[18] J. Zhao, J. Feng, G. Chen, Q. Liu, G. Hu, K. Pavol, P. Alexander, Structure analysis of loratadine, Chin. J. Anal. Chem. 31 (2003) 311–314.

[19] N.R. Pedersen, J.B. Kristensen, G. Bauw, B.J. Ravoo, R. Darcy, K.L. Larsen, L.H. Pedersen, Thermolysin catalyses the synthesis of cyclodextrin esters in DMSO, Tetrahedron Asymm. 16 (2005) 615–622.

[20] J.A. Pierce, R.S. Jackson, K.W. Van Every, P.R. Griffiths, H. Gao, Combined deconvolution and curve fitting for quantitative analysis of unresolved spectral bands, Anal. Chem. 62 (1990) 477–484.

[21] V.A. Lórenz-Fonfria, E. Padros, Curve-fitting of Fourier manipulated spectra comprising apodization, smoothing, derivation and deconvolution, Spectrochim. Acta A: Mol. Biomol. Spectrosc. 60 (2004) 2703–2710.